GEOPHYSICAL TRANSACTIONS 1997
Vol. 41. No. 1-2. pp. 65-94

Modelling the history of burial, temperature, and hydrocarbon generation of sedimentary basins. Application to the Aars-1A well

Peter Klint JENSEN*

The history of burial and subsurface temperature is calculated for the Danish well Aars-1A using simple analytical expressions. Compaction of the sedimentary sequences is taken into account. Vitrinite reflectance and hydrocarbon generation are simulated using a general chemical simulation model. The model is flexible with regard to modifications of chemical reactions. A method for calculating the heat flow history by inversion of measured vitrinite reflectance values is suggested. 1-D basin modelling is performed for the Danish well Aars-1A. The uncertainty of the calculated heat flow (relative to the present heat flow) is 25%, 100 mill. years ago. Before that time the uncertainty increases further. The hydrocarbon generation of the F-III Member of the Fjerritslev Formation is calculated using the heat flow history derived from geodynamic modelling.

Keywords: burial history, sedimentation, compaction, geothermics, maturity, vitrinite reflectance, hydrocarbon generation, simulation

1. Introduction

The ultimate goal of basin modelling is to calculate the amount of hydrocarbons generated in source rocks through time and to predict accumulations in reservoirs. The basic principles of basin models are given in YÜKLER et al. [1978], UNGERER et al. [1984] and CAO and LERCHE [1986]. A simple

* Department of Geology and Geotechnical Engineering, Technical University of Denmark, byg. 204, DK-2800 Lyngby, Denmark

Manuscript received (revised version): 2 January, 1995

one dimensional computer model was presented in JENSEN et al. [1985]. This model is able to calculate the history of 1) burial including compaction of sedimentary sequences, 2) formation temperatures, 3) vitrinite reflectance; however it is not suitable for calculating hydrocarbon migration. The model is based mainly on analytical expressions some of which are so simple that they can be used in connection with hand calculations. The model was used in a basin model study of the Aars-1A well [JENSEN et al. 1985].

In the present study a general model for simulating chemical reactions is implemented in the above mentioned 1D-basin model. Chemical reactions are traditionally simulated by deriving analytical expressions for the production rates of species. Although in certain cases the expressions may be solved analytically, in most cases they are solved numerically. Despite the analytical method being computationally efficient it is also time consuming and non-flexible. Thus, the introduction of more reactions needs re-evaluation of the analytical expressions and re-programming. SØRENSEN, STEWART [1980] showed that modelling of chemical reactions can also be performed by applying a general computation scheme with a flexible input data procedure. Reactions are specified in the input data file. This paper describes the application of the general chemical simulation method to kerogen transformation chemistry. It is shown that modification of the model by BURNHAM, SWEENEY [1989] is necessary for obtaining reasonable vitrinite reflectance values.

Past heat flow is traditionally calculated by repeated forward modelling. The assumed heat flow function is modified until there is reasonable accordance between calculated and measured vitrinite reflectance values. [LERCHE et al. 1984, LERCHE 1988a and 1988b]. Although useful results have been obtained with forward modelling there are a number of assumptions which have not been addressed, e.g. no rules are given for the choice of heat flow function, a method which determines the number of free variables is needed, the chosen function may be either too stiff or too soft. If the function is too stiff there may be cases where a rapid change of heat flow, e.g. in connection with intrusions or hydrothermal activity, cannot be satisfactorily simulated; if it is too soft the inverted heat flow history may fluctuate due to uncertain vitrinite reflectance measurements.

In this study an inversion procedure is suggested in which a piece by piece linear heat flow function is constructed on the basis of the measured vitrinite reflectance values and their uncertainties. Alternative heat flow

functions which all result in simulated vitrinite reflectance values close to measured values, are derived.

In the following the mathematical background is given for 1-D basin modelling.

2. Burial history

Sedimentary sequences are often divided into a number of formations each with a distinct lithology. Looking at a particular formation it may be reasonable to assume that the layer resulted from a continuous and steady sedimentation process. During burial the sediments are compacted due to rearrangement of the grains and of diagenesis. The grains themselves are considered incompressible. In due course the formation water occupying the pore volume escapes the diminishing pores. Empirical observations have shown that sediments often compact with the porosity decreasing exponentially with depth [ATHY 1930]. Each formation has its own characteristic exponential function. Limitations to this approach will be discussed below. The mathematical formulation of burial history including compaction, given here, is based on the principle of conservation of the solid particle mass. The sediment volume, not occupied by solid particles, is assumed to be filled with water. Once the movement and the compaction of the solid particles are given, the movement of the water may be readily found since the water just occupies the volume left over by the solid particles.

The following description is divided into two parts: the first part discusses the derivation of equations for the surface layer, the second describes underlying layers.

The sedimentation process of a surface layer may be regarded as a flow of solid particles relative to the surface, towards the depth. The rate at which solid mass is added to the surface is assumed constant from time $t=0$, when the sedimentation process started. It is assumed that the lithology and the porosity profile of the layer are constant in time during sedimentation. This means that any lump of sediment experiences equivalent burial paths. Analytical equations of the burial history of a surface layer including compaction may be deduced by considering conservation of the solid particle mass. The particles are packed with depth. This is expressed by increasing density of the solid with depth. The density is calculated as the mass of solid, per total volume of sediment, including water. The flow of compacting solid

particles may then be regarded as analogous to the flow of a compressible fluid. A differential equation may be derived from which the relation between time and depth can be determined [HUTCHINSON 1985 and JENSENet al. 1985];

$$t(z) = \frac{1}{v_0(1-\Phi_0)}\left[z + \frac{\Phi_0}{a}\left(e^{-az} - 1\right)\right] \tag{1}$$

where $t(z)$ is the time it takes a sediment grain to reach depth z, Φ_0 is the surface porosity, a is the compaction coefficient determining the compaction of sediments:

$$a = -\frac{1}{z}\ln\left(\Phi(z)/\Phi_0\right) \tag{2}$$

$\Phi(z)$ is the exponential porosity depth function. The surface velocity υ_0 is determined from:

$$\upsilon_0 = \frac{1}{(1-\Phi_0)t_b}\left[h + \frac{\Phi_0}{a}\left(e^{-ah} - 1\right)\right] \tag{3}$$

where the total surface layer thickness, h, is known from well information, and t_b is equal to an age date of the base of the layer, thus Eq. (1) is the expression governing the relation between time and depth for the sedimentation process including compaction. Given the depth, the time necessary for a sediment particle to reach this depth can be calculated simply form Eq. (1). If, on the other hand, the time is given the depth must be found from Eq. (1) by an iterative procedure (see Appendix A).

We now turn to layers underlying the surface layer. SCLATER, CHRISTIE [1980] showed that the following relation can be used to calculate the depth to the base of a layer z_4:

$$z_4 + \frac{\Phi_0}{a}e^{-az_4} = z_2 - z_1 + \frac{\Phi_0}{a}\left(e^{-az_2} - e^{-az_1} + e^{-az_3}\right) + z_3 \tag{4}$$

where z_1 and z_2 are respectively the depth to the top and the base of the layer at a given time, and z_2 and z_3 are respectively the depth to the top and the base of the layer at another time (see *Fig. 1*).

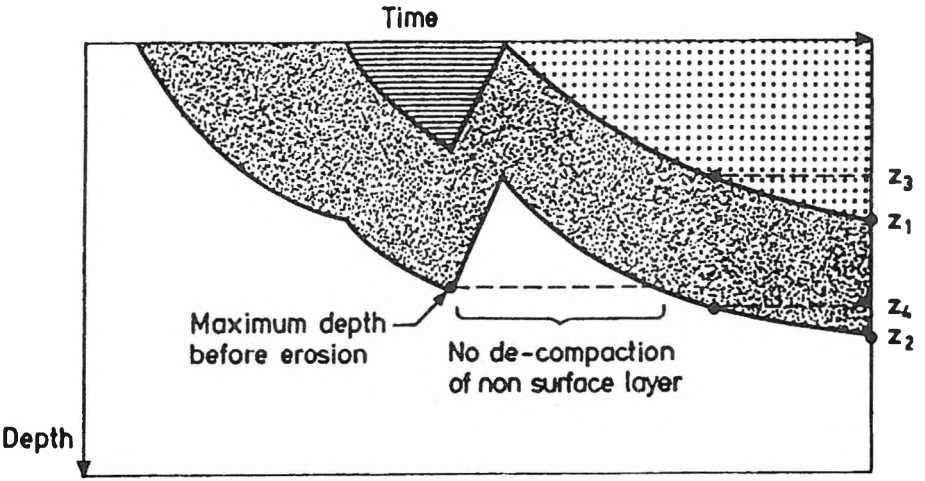

Fig. 1. Schematic drawing showing the burial history of sedimentary layers
1. ábra. Az üledékes rétegek feltöltődésének sematikus vázlata

In this equation depths z_1 and z_2 might be known from well data; z_3 may be calculated from Eq. (1); z_4 is then determined by an iterative procedure from Eq. (4), Appendix A.

The equations given above provide the foundation for calculating a multilayer sedimentation process. In sedimentary basins uplift and temporaneous erosion is a common feature. It is a general experience that sediments do not undergo much decompaction when they are uplifted. Since the elastic rebound, which is of the order of a few per cent is disregarded here, the depth history of the sediments during erosion may be modelled as a linear decrease of depth with no decompaction and with a constant uplift rate. Compaction starts when the burial depth is greater than the previous maximum depth. The maximum depth is determined by an iterative procedure. The calculations start at the present where the previous maximum depth are assumed to be zero. The formations are decompacted except during uplift. After one backstripping a first estimate of the maximum depths before erosion is calculated and the time interval with no decompaction of the formations is determined (Fig. 1). The process is repeated until the maximum depths are determined with confidence and the final estimate of the burial history is thus determined.

3. Formation temperature through time

Steady state formation temperature is calculated analytically for a given surface temperature and a given heat flow. Heat production and transport of heat by water and grain movements are not considered. The conductivity is a function of the depth dependent porosity. The conductivity function considered is

$$K = K_F + (1-\Phi)^2 (K_S + pC - K_F) \tag{5}$$

This equation is due to ROBERTSON [1979]. The conductivity is a function of fluid conductivity K_F, solid conductivity K_s for zero content of quartz, and quartz content p (percentage). The influence of the quartz content, p, is governed by multiplying by C which is a constant for each formation. Results of measurements on a large number of sedimentary rocks are given in ROBERTSON [1979] where the necessary constants in Eq. (5) may be found for different rock types. For an exponential depth decrease of porosity, and applying the conductivity given by ROBERTSON [1979] one obtains an expression for the formation temperature. For a given formation the temperature at its base $T(z_2)$ is [JENSEN et al. 1985]:

$$T(z_2) = T(z_1) + W \frac{1}{aA} \frac{1}{(K_F/A)+1} (g_1 - g_2) \tag{6}$$

where $A = K_S + pC - K_F$, $\Phi_i = \Phi_0 e^{-az_i}$, and

$$g_i = \ln \Phi_i - \tfrac{1}{2} \ln\left(\frac{K_F}{A} + (1-\Phi_i)^2 \right) - \frac{1}{K_F/A} \arctan\left(\frac{1-\Phi_i}{K_F/A} \right) \tag{7}$$

for $i = 1, 2$. Hints concerning the derivation of the above given expression are detailed in Appendix B.

4. Maturity modelling

Quantification of maturity of source rocks is often performed by measuring the vitrinite reflectance. Vitrinite reflectance is time and temperature

dependent and has been modelled by Lopatin's time-temperature index TTI [WAPLES 1980]. WAPLES related the time-temperature index to measured vitrinite reflectance values for a large number of wells world-wide. This relation can then be used to predict the maturity of source rocks by reconstructing the temperature history and calculating the time-temperature index. Other authors such as, for example, FALVEY, DEIGHTON [1982], used a time-temperature integral to calculate the vitrinite reflectance.

Although the above mentioned methods were great steps forward in this type of modelling, a number of major problems regarding these models should be noted. The concept of using maximum temperature and effective time will in some cases lead to erroneous results. In particular it is to be expected that degradation of vitrinite is a function of the whole temperature history. Another problem is that many authors do not take compaction and time dependent conductivity into account. Neither do they include the time varying surface temperature. Furthermore, only a few models include the temperature effect of water movements caused by the compaction of the sediments [YÜKLER et al. 1978 and BETHKE 1985]. For a one-dimensional case HUTCHINSON [1985] showed that the effect of water movement is important only for rapidly subsiding basins. In the case history presented below for the Aars-1A well, water movements have not been taken into account.

Founded upon the above given criticism it is not to be expected that the maturity relations given by WAPLES [1980] and FALVEY, DEIGHTON [1982] can be used with success using a basin model including compaction, time dependent conductivities, surface temperature history, and the whole time-temperature history. In this paper the chemical kinetic vitrinite maturation model by BURNHAM and SWEENEY [1989] is applied for calculating vitrinite reflectance.

5. Simulation of hydrocarbon generation

Degradation of kerogen is calculated using 35 parallel first order reactions [BURNHAM, SWEENEY 1989]. Kerogen is divided into 19 groups with different activation energies; it may be thermally degraded into H_2O, CO_2, CH_n and CH_4. The degradation of kerogen is described mathematically by first order differential equations. The activation energies and frequency factors were, according to BURNHAM, SWEENEY [1989], found from the modelling of pyrolysis experiments on samples in the laboratory and the

modelling of kerogen degradation in nature. In the latter case basin models are used to model the temperature history. BURNHAM and SWEENEY [1989] give the activation energies, the frequency factors and the initial amounts of kerogen in each group. In this study the author multiplied the original frequency factors by $0.5\ 10^{-2}$ to obtain a reasonable match between calculated and measured vitrinite reflectance values.

Since the amount of a certain species is generally the result of several reactions, the calculations may be quite complicated. However, the calculations can be systematized by utilizing matrix calculation [SØRENSEN, STEWART 1980]. The production rates of species are calculated by matrix multiplication of the reaction rates and the stoichiometric matrix.

Consider the stoichiometric matrix

$$\mathbf{v} = \begin{array}{c} \begin{array}{ccccc} S_1 & . & S_j & . & S_n \end{array} \\ \begin{pmatrix} \nu_{1,1} & \nu_{1,2} & . & . & \nu_{1,n} \\ . & . & . & . & . \\ \nu_{i,1} & . & \nu_{i,j} & . & \nu_{i,n} \\ . & . & . & . & . \\ \nu_{m,1} & . & \nu_{m,j} & . & \nu_{m,n} \end{pmatrix} \end{array} \tag{8}$$

Each row represents a chemical reaction, each column is assigned to the species S_j given above the columns, $\nu_{i,j}$ represents the stoichiometric weight of the species. By convention $\nu_{i,j}$ is negative for the elements on the left side of the reaction equation and positive for elements on the right side. The exercise is now to calculate the concentration of each species as a function of time given the initial concentrations. First, this is done by calculating the production rate R_j as a function of time. This may be the result of several reactions, and the total production rate is

$$R_j = \sum_{i=1}^{m} \nu_{i,j} \cdot r_i \tag{9}$$

where r_i is the reaction rate. The production rate is defined

$$R_j = \frac{\partial c_j}{\partial t} \tag{10}$$

where c_j is the concentration of species j, and t is the time. Equation (9) may be expressed in matrix form

$$\mathbf{R}^{\mathrm{T}} = \mathbf{r}^{\mathrm{T}}\mathbf{v}\,. \tag{11}$$

Here the transposed matrices $\mathbf{r}^{\mathrm{T}}$ and $\mathbf{R}^{\mathrm{T}}$ are column vectors. Given the initial concentrations, at a later time the concentrations can be calculated by integrating the reaction rates for each species. Integration of the non-linear differential equations is performed by LSODE, the Lawrence Livermore solver for ordinary differential equations [HINDMARSH 1980]. Simple calculation examples using matrices are given in SØRENSEN [1982].

The reaction rate is usually a function of species concentration

$$r_i = k_i \cdot \left[\prod_j c_j^{\varepsilon_{i,j}} - \frac{1}{K_i} \prod_j c_j^{\nu_{i,j}+\varepsilon_{i,j}} \right] \tag{12}$$

where $c_j = [S_j]$ is the source rock concentration of a species, $\varepsilon_{i,j}$ is an element in the reaction order matrix $\underline{\underline{\varepsilon}}$. $\varepsilon_{i,j}$, may be determined from published reaction rate expressions; k_i is the forward reaction rate constant, and K_i is the equilibrium constant. k_i may be temperature dependent

$$k_i(T) = A_i\left(T_{k,i}\right) \exp\left[\frac{E_i}{R_{Ad}} \left(\frac{1}{T_{k,i}} - \frac{1}{T} \right) \right] \tag{13}$$

where T is the temperature (Kelvin), A_i is the frequency factor at the base temperature $T_{k,i}$ (usually 25 °C), E_i is the activation energy, and R_{Ad} is Avogadro's number.

The equilibrium constant is also temperature dependent

$$K_i(T) = K_{b,i}\left(T_{K,i}\right) \exp\left[\frac{\Delta H_i}{R_{Ad}} \left(\frac{1}{T_{K,i}} - \frac{1}{T} \right) \right] \tag{14}$$

where $K_{b,i}$ is the equilibrium constant at the base temperature $T_{K,i}$ (in degrees K), ΔH_i is the reaction enthalpy. The stoichiometric matrix is here derived from the reaction kinetics given by BURNHAM, SWEENEY [1989]. The matrix is quite large therefore only the submatrix for the reactions involving water production is shown here. The stoichiometric sub-matrix is in this case

$$\mathbf{v}_w = \begin{array}{c} \begin{matrix} P_1 & . & P_8 & R_1 & . & R_8 & H_2O \end{matrix} \\ \begin{pmatrix} -1 & . & 0 & 1 & . & 0 & 1 \\ . & . & . & . & . & . & . \\ 0 & . & -1 & 0 & . & 1 & 1 \end{pmatrix} \end{array} \tag{15}$$

where $P_1 \ldots P_8$ are the kerogen precursors for water, and R_1–R_8 are the kerogen residuals. The rows of the stoichiometric matrix express the transformation of the water kerogen precursor to kerogen residual and water. The reaction order matrix is

$$\underline{\underline{\varepsilon}}_w = \begin{array}{c} \begin{matrix} P_1 & . & P_8 & R_1 & . & R_8 & H_2O \end{matrix} \\ \begin{pmatrix} 1 & . & 0 & 0 & . & 0 & 0 \\ . & . & . & . & . & . & . \\ 0 & . & 1 & 0 & . & 0 & 0 \end{pmatrix} \end{array} \tag{16}$$

Applying the equations (15) and (16) in equation (12) and using $K_i = \infty$ one obtains the reaction rates $r_i = k_i[P_i]$, $i = 1, \ldots, 8$, which is a first order reaction as expected. The matrices for the chemical reactions producing CO_2, CH_n, and CH_4 are similar to matrices (15) and (16).

The reaction rate r_i is computed from Eq. (12) with the equilibrium constant being infinity. The forward rate constant is calculated from Eq. (13).

Multiplication of the reaction rate vector and the stoichiometric matrix, Eq. (11), results in the production rate vector for:

$$\begin{pmatrix} R_{P_1} \\ . \\ R_{P_8} \\ R_{R_1} \\ . \\ R_{R_8} \\ R_{H_2O} \end{pmatrix} = \begin{pmatrix} r_1 \\ . \\ r_8 \end{pmatrix} \begin{array}{c} \begin{matrix} P_1 & . & P_8 & R_1 & . & R_8 & H_2O \end{matrix} \\ \begin{pmatrix} -1 & . & 0 & 1 & . & 0 & 1 \\ . & . & . & . & . & . & . \\ 0 & . & -1 & 0 & . & 1 & 1 \end{pmatrix} \end{array} \tag{17}$$

The last element, R_{H_2O}, in the production rate vector is the total water production rate. The species concentration as a function of time may then be calculated by integrating the production rate vector, given the initial concentrations.

6. Estimation of past heat flow

Heat flow history may be calculated by inversion of vitrinite reflectance depth profile measurements [MIDDLETON 1982, LERCHE 1988a and 1988b]. In these papers variables of an initially assumed heat flow function are adjusted until there is a reasonable match between calculated and measured vitrinite reflectance values. However, no rules are given for the choice of function or its number of degrees of freedom. A procedure for calculating past heat flow as a piece by piece linear function is given in the following. Sedimentation age increases with depth. *Figure 2* illustrates a simple approach to inverting the vitrinite reflectance values. A piece by piece linear heat flow function is used (Fig. 2). The figure shows three co-ordinate systems: the uppermost is used for the heat flow history, the right one is used for the vitrinite reflectance values, the lower left co-ordinate system is for the burial history. The linear segment of the heat flow history which is valid for the most recent time, has an endpoint at the present and the other endpoint at the age of the uppermost

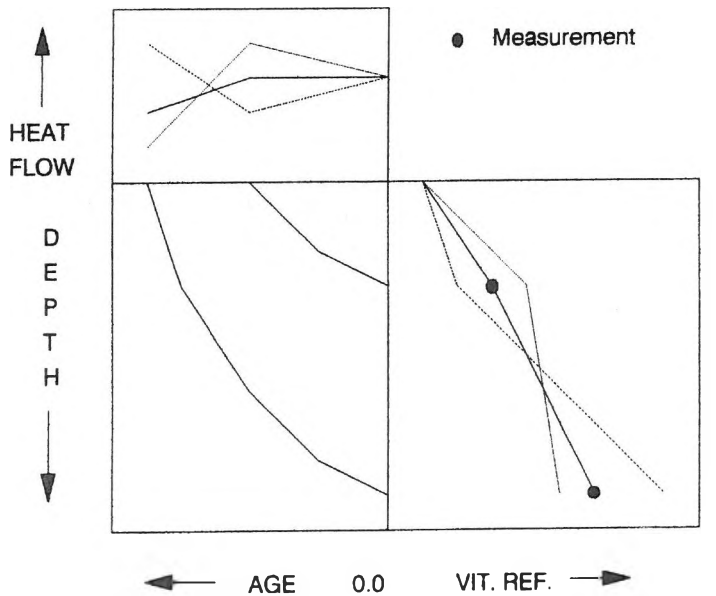

Fig. 2. The lower left co-ordinate system shows the burial history for two vitrinite reflectance samples. The reflectance values are given in the lower right co-ordinate system. Three heat flow functions are given in the uppermost coordinate system

2. ábra. A bal alsó koordináta rendszer a feltöltődés menetét mutatja két vitrinit reflektivitási mintára. A reflektivitás értékek a jobb alsó koordináta rendszerben láthatók. A legfelső koordináta rendszer három alternatív hőáram függvényt mutat

sample. The next (older) segment is valid for the time span between the age of the uppermost sample and the next deeper sample. In this case the number of degrees of freedom for the heat flow function is equal to the number of samples. For the first segment the endpoint at the present has a heat flow value equal to the present day heat flow value; the heat flow value at the other endpoint may be calculated iteratively by simulating the uppermost vitrinite reflectance value. The heat flow function may be continued further back in time provided that deeper samples are available. The next segment may be calculated similarly using the next deeper sample.

Uncertainties of the vitrinite reflectance values lead to uncertainties in the inverted heat flow function. This is illustrated in Fig. 2, where three heat flow functions are shown. The function which leads to a close match between simulated and measured vitrinite reflectance values has already been discussed. The other two functions are determined such that their corresponding calculated vitrinite reflectance values are at the outer limit of the error bars for the measured vitrinite reflectance values (Fig. 2). As the depth distance of the samples becomes small the uncertainty of the calculated heat flow becomes large, and even unrealistically large fluctuations may be obtained. This problem may be solved by enlarging the distances between vitrinite reflectance measurements. Enlarging the distances means that the segments of the heat flow function cover larger time intervals. Since the heat flow history is constructed by line segments beginning at the most recent time and progressing back in time, the uncertainty of a segment is dependent on the uncertainty of the preceding segment, but not on the following one. The uncertainty is thus increasing back in time. To avoid steadily larger fluctuations of the calculated heat flow backwards in time the length of the line segments has to be increased.

7. Basin modelling of the Aars-1A well

The basin model described above is used to simulate hydrocarbon generation for the Danish well Aars-1A.

The Aars-1A well is situated in the Danish Sub-basin, *Fig. 3*. A subdivision in stage/formation/member and a brief summary of the regional setting are given in THOMSEN et al. [1987]. The post Chalk Group erosion is here assumed to be 600 m [JAPSEN 1993]. The potential source rock is the F-III Member of the Fjerritslev Formation, *Fig. 4* [ØSTFELDT 1986]. The age

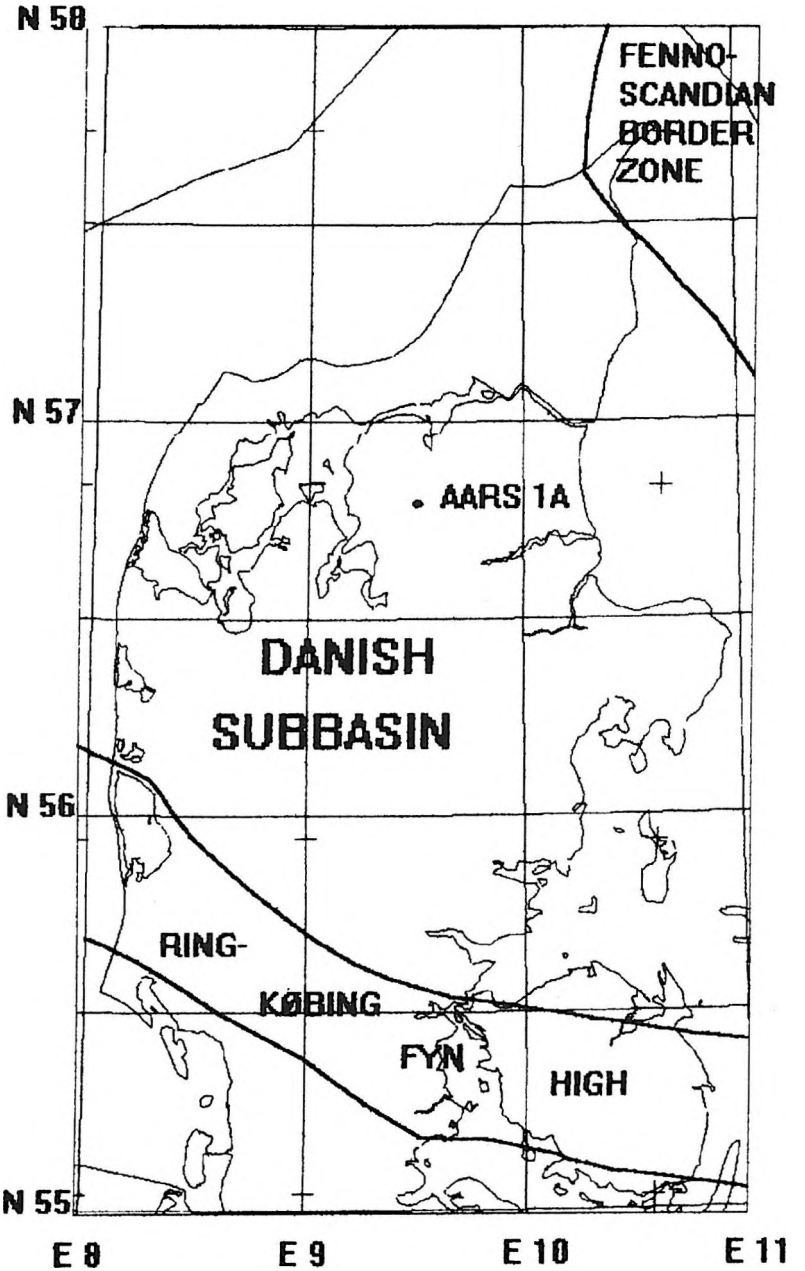

Fig. 3. Map of the Danish Sub-basin and location of the Aars-1A well [after MICHELSEN 1982]

3. ábra. A dán al-medence térképe és az Aars-1A mélyfúrás helyzete [MICHELSEN 1982 nyomán]

dates are based on HAQ et al. [1987]. The total time span of 210 mill. years is divided into 13 events comprising time intervals of sedimentation or erosion. The compaction constants are determined from assumed surface porosities and from a semi-log plot of porosities versus depth for the

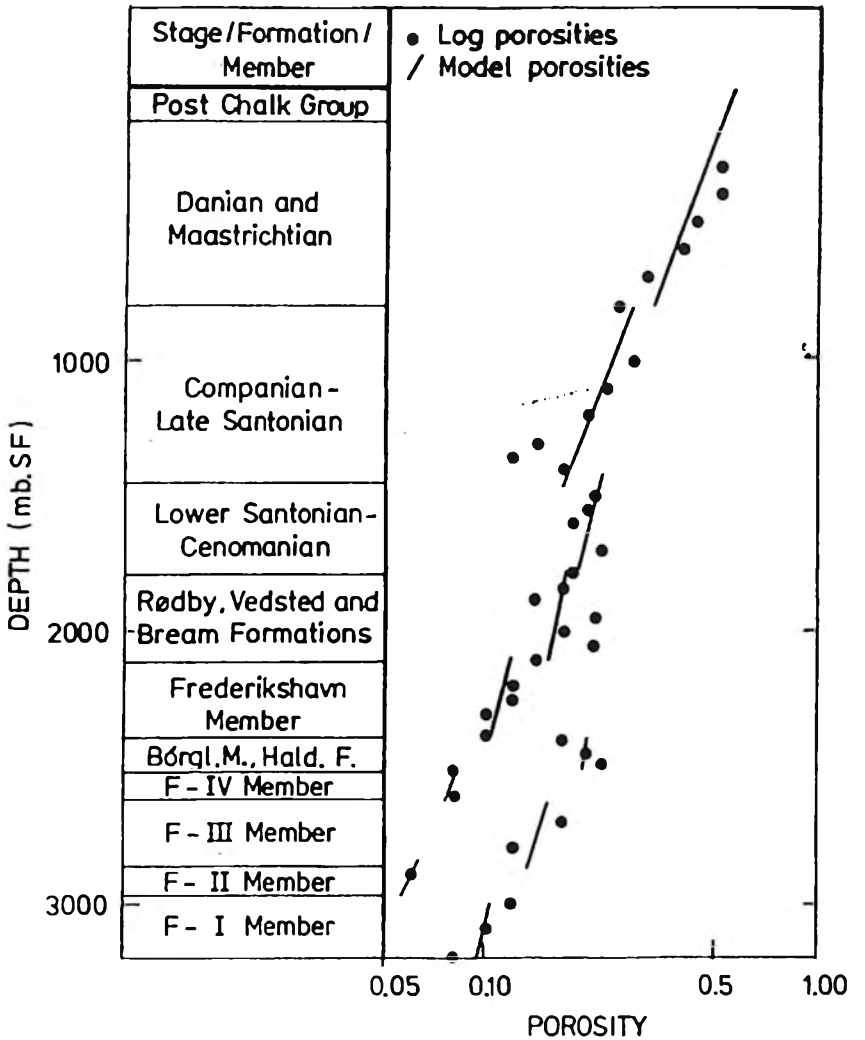

Fig. 4. Log derived and model porosities as a function of depth. The straight lines are exponential function approximations used in the modelling

4. ábra. Karotázs mérésekből levezetett és modell-porozitás értékek a mélység függvényében. Az egyenes vonalak a modellezés során használt exponenciális függvény közelítő értékeit adják meg

individual formations (Fig. 4). The calculated burial history is shown in *Fig. 5.*

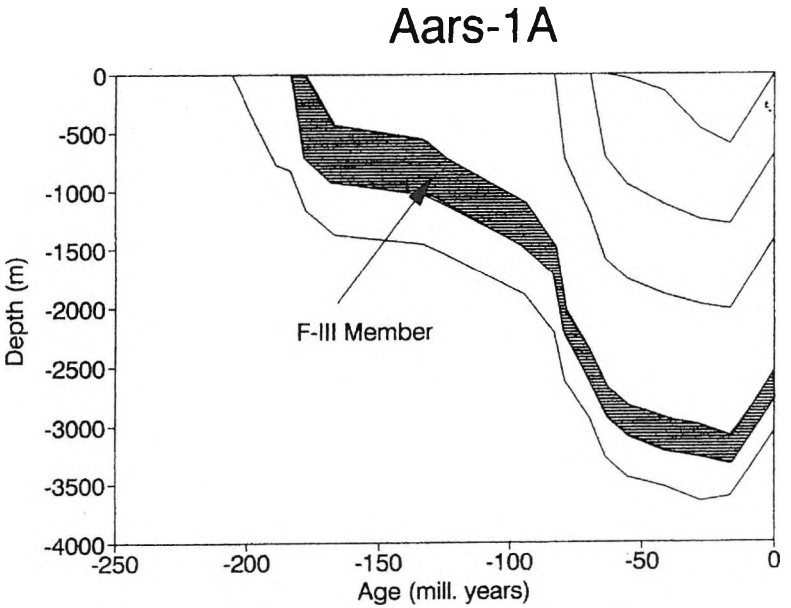

Fig. 5. Simulated burial depth as a function of time including compaction of the sediments

5. ábra. Szimulált feltöltődési mélységek az idő függvényében, figyelembe véve az üledékek kompakcióját is

The sediment surface temperatures (*Fig. 6*) are given by BUCHARDT [1978] for the period back to 60 mill. years. Data for older times were obtained after personal communication with B. BUCHARDT**. The thermal constants determining the conductivities of the rocks using Robertson's model, Eq. (5), are shown in Table 3 in JENSEN et al. [1985]. These constants are found stepwise. First a set of constant is found from figures given by ROBERTSON [1979] for each lithology knowing the porosity and the quartz content. Based on this conductivity model the input heat flux is adjusted to obtain a calculated temperature profile as close as possible to the measured temperature profile. The temperature profile was measured 1 1/2 years after

** Institute of Historical Geology and Palaeontology, University of Copenhagen, Østervoldgade 10, DK-1350 Copenhagen K, Denmark

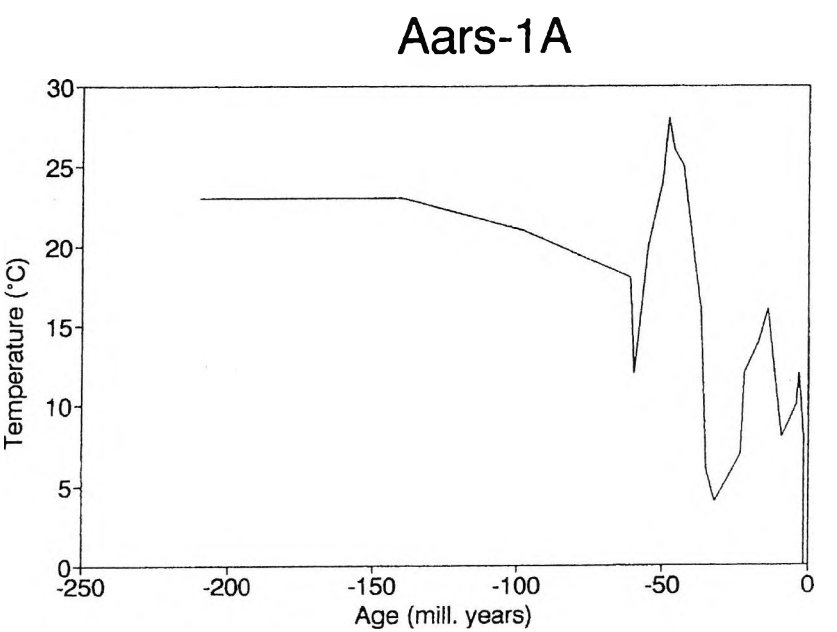

Fig. 6. Surface temperature as a function of time. The surface temperature is due to BUCHARDT [1978]

6. ábra. Felszíni hőmérséklet az idő függvényében BUCHARDT adatai alapján [1978]

cessation of the circulation [BALLING1986] and it is expected that the measured temperatures are within ± 1–2 °C of the true formation temperature. In this way the present heat flow is estimated to be 55 mWm^{-2}, which value is slightly lower than the mean value of 60 mWm^{-2} estimated for the area based on conductivity measurements and temperature logging, BALLING [1986]. A better match (*Fig. 7*) is then obtained by adjusting the constant C in Robertson's conductivity equation, Eq. (5).

The heat flow history calculated by VEJBÆK [1989] is utilised to calculate the formation temperature history (Fig. 7). The heat flow history is based on geodynamic modelling. LARSEN [1986] estimated the formation temperature of the Gassum Formation (just below the Fjerritslev Formation) to be above 130 °C in the early Tertiary. Oxygen $^{18}O/^{16}O$ measurements of formation water were used. The estimate is in accordance with the simulation shown in *Fig. 8.*

The 1-D-basin model is run applying the kinetics by BURNHAM, SWEENEY [1989]. Calculation of the vitrinite reflectance is based on the calculated composition of the residual kerogen as described by BURNHAM, SWEENEY

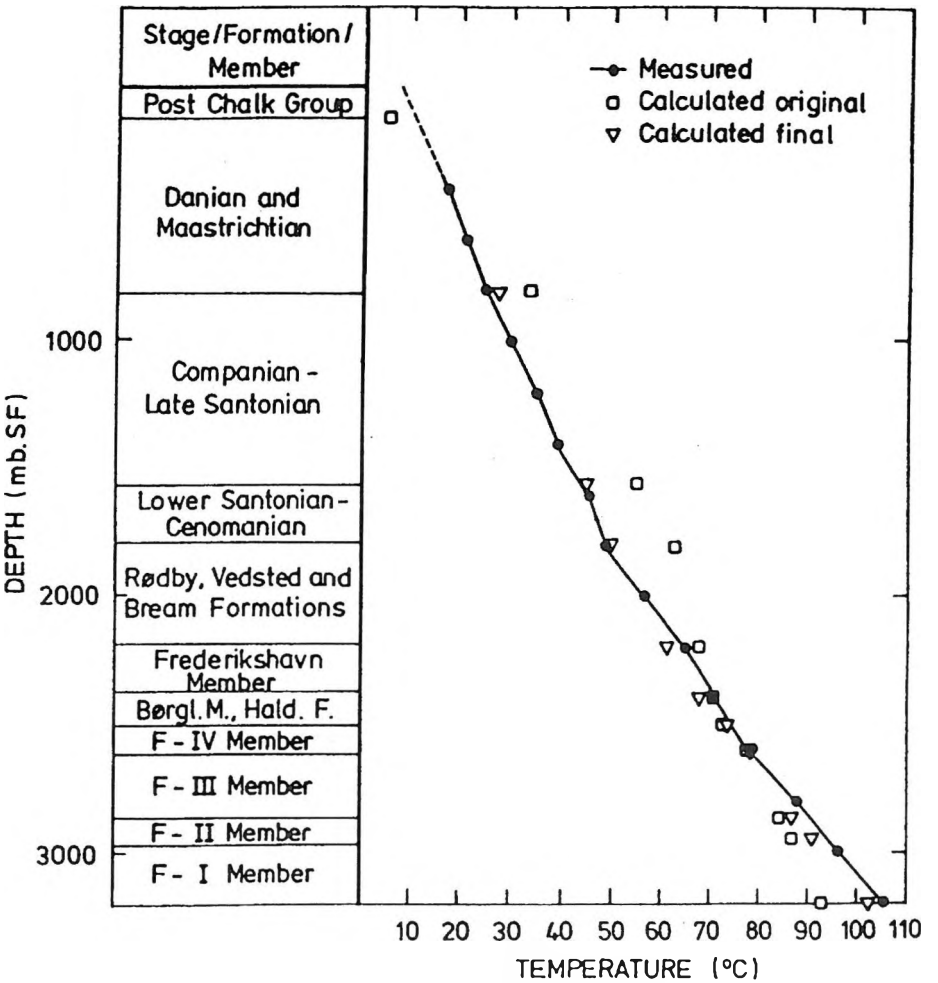

Fig. 7. Measured [BALLING 1986] and calculated temperatures for the Aars-1A well
7. ábra. Mért [BALLING 1986] és számított hőmérséklet értékek az Aars-1A mélyfúrásra

[1989]. A too low calculated vitrinite reflectance value 1.5 % R_0 at the bottom of the well was obtained (*Fig. 9*). A parameter study showed that realistic heat flow histories could not be obtained with the kinetic parameters given by BURNHAM, SWEENEY [1989]. It is necessary to adjust the kinetic model to avoid unrealistic heat flow histories. A reasonable match (Fig. 9) is obtained using the geodynamic heat flow model [VEJBÆK 1989] and the surface

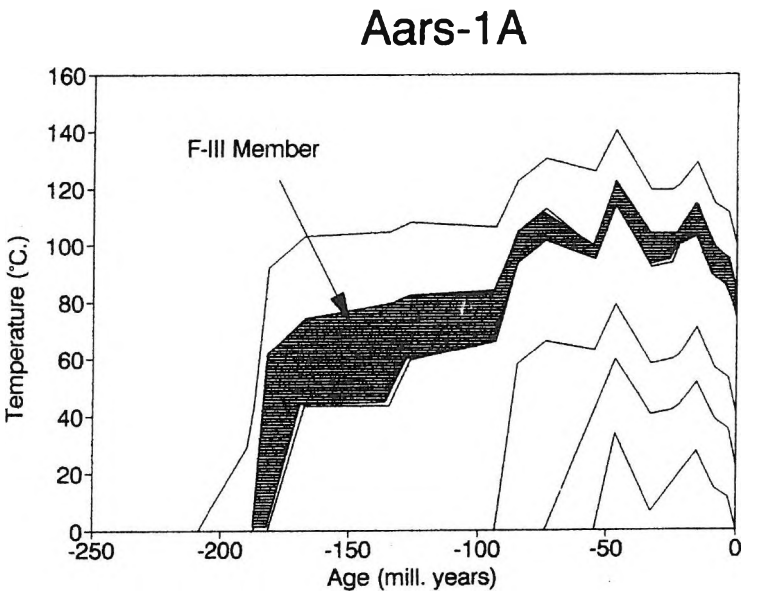

Fig. 8. Simulated formation temperatures as a function of time
8. ábra. Szimulált formáció hőmérsékletek az idő függvényében

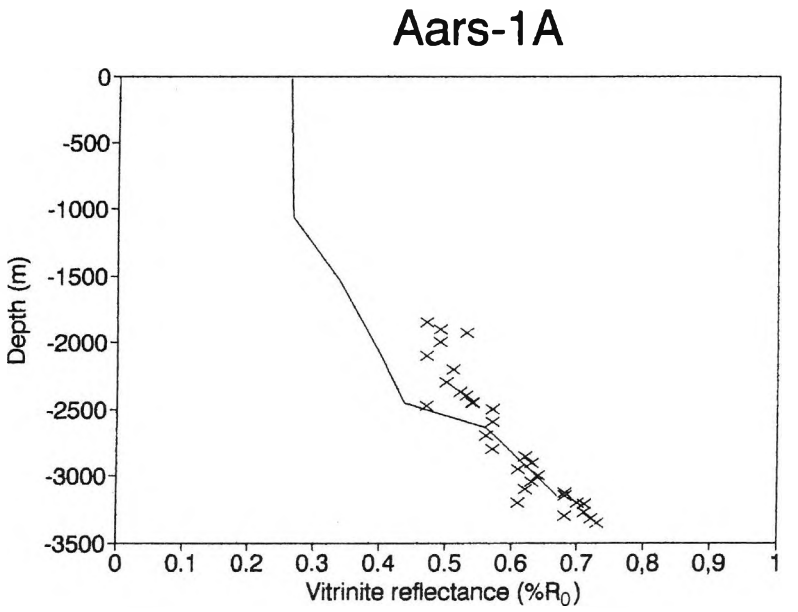

Fig. 9. Measured [THOMSEN 1984] and calculated vitrinite reflectance values
9. ábra. Mért [THOMSEN 1984] és számított vitrinit reflektivitási értékek

temperature by BUCHARDT [1978] when the frequency factors given by BURNHAM, SWEENEY [1989] are multiplied by $0.5\ 10^{-2}$.

The computed vitrinite reflectance values as a function of time are shown in *Fig. 10.* Only the lower part of the Fjerritslev Formation reaches vitrinite reflectance values above 0.6% R_0, which is often regarded as the critical value for onset of oil generation.

Also the recent total oil, gas, water, and carbon dioxide generation of the F-III Member was calculated. According to ØSTFELDT [1986] this rock unit has the most promising potential source rock in the area. LECO-Rock Eval data for the Aars-1A well are reported by ØSTFELDT [1986], *Table I.* The production index (*PI*) shows a mean value around 9%. The bitumen content (*S*1) is around 0.25 (mg oil/g of rock) and the total organic carbon content (*S*2) is around 2.4% (g organic carbon/g of rock) which is equivalent to about 1% (g oil/g organic carbon). The calculations show that 14% of the potential of light hydrocarbons ($CH_{1.7}$) has been generated, methane has not yet been generated. The calculated production index is:

$$PI = \frac{\gamma f_f}{\gamma + \delta} \tag{18}$$

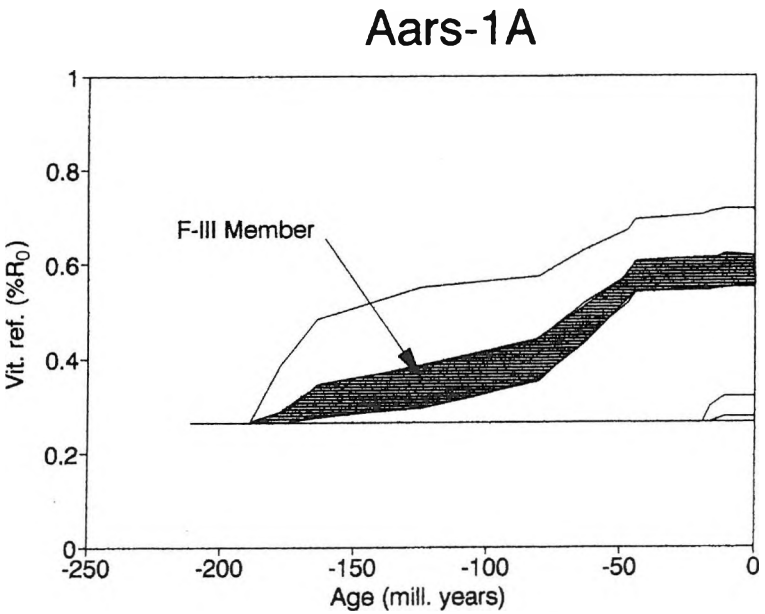

Fig. 10. Simulated vitrinite reflectance values as a function of time
10. ábra. Szimulált vitrinit reflektivitási értékek az idő függvényében

Meter	TC	TOC	T_{max}	S1	S2	PI	HI
2600	6.41	5.05	436	.31	4.37	.07	87
2650	5.02	3.60	427	.72	3.50	.17	97
2700	2.87	1.76	429	.38	3.27	.10	186
2750	2.39	1.63	432	.19	1.65	.10	101
2800	2.27	1.60	432	.24	2.39	.09	150
2855	3.19	1.89	435	.14	1.89	.07	100

Table I. LECO-Rock Eval data from cutting samples of the F-III member of the Fjerritslev Formation at the Aars-1A well [ØSTFELDT 1986]

I. táblázat. LECO-Rock Eval adatai a Fjerritslev formáció F-III tagjából származó metszetekből az Aars-1A mélyfúrásból. [ØSTFELDT 1986]

where γ and δ are the fractions of initial carbon that ultimatly may be removed from the initial kerogen as CH_n and CH_4 respectively, and f_c is the fraction of carbon converted to CH_n. The conversion ratios for H_2O, CO_2, CH_n, and CH_4 are defined: $F_\alpha = [H_2O]/[H_2O]_0$, $F_\beta = [CO_2]/[CO_2]_0$, $F_\delta = [CH_n]/CH_n]_0$, and $f_C = [CH_4]/[CH_4]_0$, where in each case the index 0 indicates initial concentrations. In the calculation example γ is 12.5% and δ is 1% [BURNHAM, SWEENEY 1989], and f_C is here calculated to be 14% which leads to a calculated value for the production index equal to 0.13. The calculated production index may be compared with the measured production index $S_1/(S_1+S_2)$ where S_1 is the volatile hydrocarbons and S_2 is the hydrocarbon derived from kerogen pyrolysis. The calculations as well as the measurement show that a small amount of oil has been generated and only a small fraction of the potential has been transformed. Although the hydrocarbon generation is small in the Aars-1A well it may be higher in areas of the basin where the burial is deeper.

A sensitivity study is performed to see the effect of the assumed linear heat flow function. The results are summarised in *Table II*. The preferred heat flow function linearly increases from 55-67 mWm^{-2} [VEJBÆK 1989]. The simulations show that onset of hydrocarbon generation occurred quits suddenly (within 500,000 years). The onset most likely occurred within the last 30 to 18 mill. years.

Application of the geodynamically calculated heat flow function and the modified kinetic model leads only to a rough match between calculated and

Heat Flow (mWm^{-2})	Onset of Oil Gen. mill. years	Vit. Ref. % R_0	f_c
40	no onset	0.60	0.00
50	18	0.62	0.10
67	**30**	**0.64**	**0.14**
70	37	0.65	0.15
80	50	0.68	0.18

Table II. Parameter study varying the assumed linear heat flow function. For all cases the present heat flow is 55 mWm^{-2}. The F-III Member of the Fjerritslev Formation is considered. Vitrinite reflectance and the fraction of CH_n production, f_c is calculated for the present time. The preferred model is in bold letters

II. táblázat. Paraméter vizsgálatok a feltételezett lineáris hőáram függvény változtatásával. Mindegyik esetben a jelenlegi hőáram 55 mWm^{-2}. A Fjerritslev formáció F-III tagját vizsgálták. A vitrinit reflektivitást és a CH_n termelés frakcióját, az f_c-t a jelenlegi időpontra számították. A kedvezőnek ítélt modellt vastag betű jelöli

measured vitrinite reflectance values (Fig. 9). Refinement of the match is performed by adjusting the heat flow history applying the above described inversion method. Vitrinite reflectance measurements are performed from 10 to 186 times at each depth [THOMSEN 1984]. The standard deviation for each measurement is generally a little less than 10%. In the inversion procedure a general value of 10% has been used. As there are no vitrinite reflectance measurements within the Chalk Group, only a linear heat flow segment can be estimated for that period (corresponding to the base of layer 6). The present day heat flow is assumed to be error-free. Alternative inverted heat flow histories are shown in *Fig. 11* together with the heat flow history calculated by geodynamic modelling [VEJBÆK 1989]. The alternatively inverted heat flow histories lead to calculated vitrinite reflectance values which match measurements within 10%. Only the most recent parts of the heat flow function, which fall within realistic heat flow values, are shown. The inverted heat flow function can thus only be estimated with reasonable error limits 100 mill. years back in time. The heat flow values show higher values than for the heat flow function derived from geodynamic modelling. Due to the limited extent, back in time, the heat flow function derived from geodynamic modelling is used for kinetic modelling.

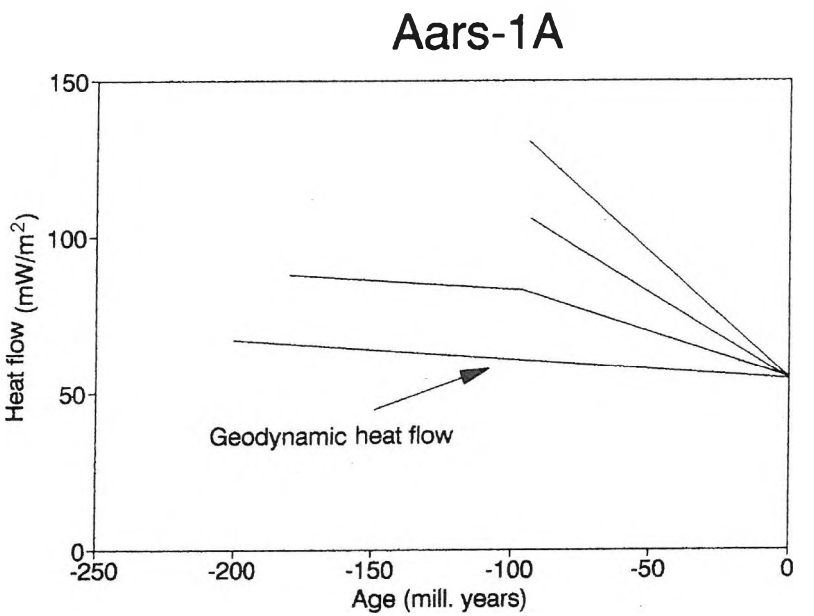

Fig. 11. Alternative heat flow histories calculated by inversion of measured vitrinite reflectance data. The thermal history from geodynamic modelling by VEJBÆK [1989] is also shown

11. ábra. A mért vitrinit refelektivitási adatok inverziójával számított alternatív hőáram változások és a VEJBÆK [1989]-féle geodinamikai modellezésből eredő termikus történet

8. Discussion

A major limitation of the analytical expressions for the burial history of sedimentary sequences outlined in this paper is the predefined porosity–depth function. Although such relations have been used widely in the literature they cannot adequately describe the porosity conditions in overpressured shales. In these zones, compaction ceases because formation water is trapped due to the low permeability. Pre-defined compaction curves can therefore only roughly estimate the natural conditions.

The equations for formation temperature are developed for stationary conditions. This condition is only partly valid since surface temperature and heat flow may vary with time. Also variations of the sedimentation rate cause transient effects. This may be important for rapidly subsiding basins [HUTCHINSON 1985].

Determination of rock heat conductivities is connected with high uncertainties, but a close match of simulated and measured formation temperatures can be obtained despite inaccuracies of the conductivity model. This is done by adjusting the assumed present heat flow model. Basin modelling is therefore not particularly sensitive to the accuracy of the heat conductivity model since a satisfactory match between simulated and measured temperatures can be obtained.

The equations concerning the history of burial and temperature presented here are attractive firstly because the approach is simple and secondly because the results, for 1-D modelling, may be as accurate as more advanced modelling including compaction-driven ground water flow. In advanced 1-D modelling only vertical movements are allowed. This restriction is seldom fulfilled in sedimentary basins [see BETHKE 1985]. Improved estimates of burial and temperature history of sediments can only be obtained by two- or three-dimensional simulations including water movements.

In an earlier study JENSEN [1988] it was shown that if one applies the kinetic model by TISSOT et al. [1987] and a thermal history for the Aars-1A well including compaction, variation of conductivity with time, and a surface temperature history they lead to transformations of the kerogen that are much too high when compared with measured transformation ratios. There may be several reasons for the necessity of modifying the published kinetic models. First of all there may be differences in the chemical composition between the kerogen at the Aars-1A well and the kerogen considered by BURNHAM, SWEENEY [1989] and TISSOT et al. [1987]. Second, there are differences in the basin models used by the different authors. If a basin model is used with kinetic parameters originating from calibrations using a basin model that do not take compaction or surface temperature into account, considerable errors may arise.

The kinetic model given by BURNHAM, SWEENEY [1989] can adequately simulate the transformation ratios observed in the Aars-1A well providing adjustments of the frequency factors are made as described above. To test the predictive force of the kinetic model more well data must be included.

Although the matrix method ensures a flexible input scheme the computing time is high. The steady improvement in the speed of computers makes the matrix method even more attractive in the future.

The inversion method described above is attractive since it avoids unrealistic fluctuations of the calculated heat flow history which are caused by the uncertainty of the vitrinite reflectance measurements. However, the

fluctuations may also be caused by the kinetic model itself, because the kerogen is assumed to be described by a limited number of activation energies.

9. Conclusions

Burial, compaction, and temperature history of sediments may be described by a set of easily solvable equations. The matrix method for calculating chemical reactions by SØRENSEN, STEWART [1980] has successfully been implemented in a chemical kinetic model, the model being flexible in terms of changes of species in the input scheme. Thus, re-evaluation of equations and re-programming are avoided if new species are introduced. However, the matrix approach is not as efficient concerning computing time as the traditional analytical approach.

A 1–D basin model study was performed for the Danish well Aars-1A. The heat flow history was first calculated by inversion of measured vitrinite reflectance data. Due to the uncertainties of the measurements the resulting heat flow history fluctuates especially when the distance between vitrinite reflectance samples is small. If the distance between the samples is increased, it diminishes the fluctuations thereby making the estimated heat flow more reliable. However, this is at the cost of the worsening of the time resolution.

On the basis of the calculated formation heat conductivities the measured temperature depth profile is simulated with good agreement when the present day model heat flow is 55 mWm^{-2}. Vitrinite reflectance values and hydrocarbon generation is simulated satisfactorily using the heat flow history derived from geodynamic modelling [VEJBÆK 1989] and using chemical kinetic data from BURNHAM, SWEENEY [1989] with the modification that all frequency factors are multiplied by 0.5×10^{-2}.

The maturity history for a number of formations is calculated using the heat flow history from geodynamic modelling. The vitrinite reflectance of the F-III Member of the Fjerritslev Formation was close to 0.6% R_0 75 mill. years b.p. and has not increased much since that time. Calculations show that a minor amount of oil has been generated in the last 30–18 mill. years, and only a very small amount of gas has been generated.

Acknowledgement

Thanks are given to Zahari ZLATEV who guided us through the running of the LSODE differential equation solver.

Appendix A

Derivation of burial history equations

The Newton Method

Solving the two transcendental equations (Eqs. 1 and 4) is equivalent to solving the equation $f(z)=0$. The two equations can be transformed to this form by isolating a zero on the right side of the equations. The Newton method [BRONSTEIN, SEMENDJAJEV 1963, p. 123] assumes that if z_i is an approximation to the solution, then

$$z_{i+1} = z_i - \frac{f(z_i)}{f'(z_i)} \tag{A1}$$

is a new and better approximation.

This new approximation may then be used instead of z_i in Eq. (A1) to give an even better approximation. The process converges providing the function is monotonic.

Surface layer

Given the time t in Eq. (4) the corresponding depth z must satisfy the equation

$$\frac{1}{\upsilon_0(1-\Phi_0)}\left[z + \frac{\Phi_0}{a}\left(e^{-az} - 1\right)\right] - t = 0 \tag{A2}$$

The iteration procedure, Eq. (A1), is then

$$z_{i+1} = z_i - \frac{\left[z_i + \frac{\Phi_0}{a}\left(e^{-az_i} - 1\right)\right] - t}{\left[1 - \Phi_0 e^{-az_i}\right]} \tag{A3}$$

It is easily seen by differentiation with depth z, that $f(z)$ is monotonic, knowing that $\Phi_0 < 1$.

Non-surface layers

The unknown depth, z_4, is to be found in Eq. (4) given the depths z_1, z_2, and z_3. The function f in Eq. (A1) is

$$f(z_{4i}) = z_{4i} - z_2 + z_1 - z_3 - \frac{\Phi_0}{a}\left[e^{-az_2} - e^{-az_1} + e^{-az_3} - e^{-az_{4i}}\right] \qquad \text{(A4)}$$

and the derivative

$$f'(z_{4i}) = 1 - \Phi_0 e^{-az_{4i}} \qquad \text{(A5)}$$

Appendix B

The temperature profile in sediments

The expression for the steady state temperature profile, Eq. (6), in sediments with the porosity decreasing exponentially with depth and with the heat conductivity given by Robertson's equation, Eq. (5), will be deduced below. The temperature, $T(z_2)$, at the base of the formation is

$$T(z_2) = T(z_1) + W\int_{z_1}^{z_2} \frac{1}{K(z)}\mathrm{d}z \qquad \text{(B1)}$$

where $T(z_1)$ is the formation temperature at the top of the formation, W is the heat flow, and $K(z)$ is the heat conductivity. The integral, I, in Eq. (B1) may be written as

$$I = \int_{z_1}^{z_2} \frac{\mathrm{d}z}{K_F + (1-\Phi)^2\left[K_s + pC - K_f\right]} \qquad \text{(B2)}$$

Since the porosity $\rho = \rho_0 e^{-az}$ and the derivative $\mathrm{d}\rho = a\rho\,\mathrm{d}z$, the integral becomes, by shift of variable

$$I = \frac{1}{aA}\int_{\Phi_1}^{\Phi_2} \frac{\mathrm{d}\Phi}{\Phi\left[\sqrt{(K_F/A)^2 + (1-\Phi)^2}\right]} \qquad \text{(B3)}$$

where $A = K_s + pC - K_F$. The integral has now a form where an analytical solution can be found [BRONSTEIN, SEMENDJAJEV 1963, p. 302, eq. 82]:

$$I = \frac{1}{aA} \frac{1}{(K_F/A)+1} (g_1 + g_2) \tag{B4}$$

where g_1 and g_2 are defined by Eq. (17).

Appendix C

List of symbols

Explanations of symbols used in the equations are given together with units.

a = compaction coefficient, m^{-1}
A = $K_s + pC - K_F$, $Wm^{-1}K^{-1}$
A_i = frequency factor for reaction i, s^{-1}
c = species concentration, mole cm^{-3}
C = constant for each rock type governing the influence of quartz on heat conductivity, $Wm^{-1}K^{-1}$
E_i = activation energy for reaction i, J mol^{-1}
g_i = function explained by Eq. (7), dimesionless
h = thickness of surface layer at present, m
k_i = chemical reaction rate for reaction i, dimension depends on reaction
K = bulk heat conductivity of sediment, $Wm^{-1}K^{-1}$
$K_{b,i}$ = equilibrium constant at base temperature
K_F = fluid heat conductivity, $Wm^{-1}K^{-1}$
K_i = equilibrium constant, dimension depends on reaction
K_s = solid conductivity for zero content of quartz, $Wm^{-1}K^{-1}$
p = quartz content, percentage
R = production rate, mole $cm^{-3}s^{-1}$
R_{Ad} = Avogadro's constant
R' = reaction rate, mole $s^{-1}cm^{-3}$
R_0 = vitrinite reflectance, percentage
S_j = chemical species

t = time, s
t_b = age date of base of surface layer, s
T = formation temperature, K
$T_{k,i}$ = base temperature for frequency factor
$T_{K,j}$ = base temperature for equilibrium constant
υ_0 = surface grain velocity, ms^{-1}
W = heat flow, Wm^{-2}
z = depth from sediment surface, m
z_i = depth of location i, m
$\underline{\varepsilon}$ = reaction order matrix, dimensionless
ρ_m = matrix (grain) density, kg m^{-3}
ρ_{sol} = bulk solid density (mass of solid particles per volume of sediment), including water, kg m^{-3}
ΔH_i = enthalpy difference
ρ = porosity, dimensionless
ρ_i = porosity of depth z_i, dimensionless
ρ_0 = surface porosity, dimensionless
ν = stoichiometric matrix, dimensionless

REFERENCES

ATHY L. F. 1930: Density, porosity, and compaction of sedimentary rocks. AAPG Bull. **14**, 1, pp. 1–24

BALLING N. 1986: Principal uses of heat-flow data. *In*: MØLLER (ed): Twenty-five years of geology in Aarhus. Geoskrifter, No. 24. 300 p.

BETHKE C. M. 1985: A numerical model of compaction-driven groundwater flow and heat transfer and its application to the paleohydrology of intracratonic sedimentary basins. Journal of Geophysical Research **90**, B8, pp. 6817–6828

BRONSTEIN I. N., SEMENDJAJEV K. A. 1963: Taschenbuch der Mathematik. P. G. Teubner Verlaggesellschaft, Leipzig, 584 p.

BUCHARDT B. 1978: Oxygen isotope paleotemperature from the Tertiary period in the North Sea areas. Nature **275**, pp. 121–123

BURNHAM A. K., SWEENEY 1989: A chemical kinetic model of vitrinite maturation and reflectance. Geochimica et Cosmochimica Acta **53**, pp. 2649–2657

CAO S., LERCHE I. 1986: Fluid flow, hydrocarbon generation and migration: A quantitative model of dynamical evolution in sedimentary basins. Offshore Technology Conference Proceedings, Houston, Texas, Paper 5182, **2**, pp. 267–276

FALVEY D. A., DEIGHTON I. 1982: Recent advances in burial and thermal geohistory analysis. APEA, **22**. pp. 65–81

HAQ B. U., HARDENBOL J., VAIL P. R. 1987: Chronology of fluctuating sea levels since the Triassic (250 million years ago to present). Science **235**. pp. 1156–1167

HINDMARSH A. C. 1980: LSODE and LSODE1, two new initial values ordinary differential equation solvers. ACM-Signum, Newsletter **15**, 4, pp. 10–11

HOOD A., GUTJAHR C. C. M., HEACOCK R. L. 1975: Organic metamorphism and the generation of petroleum. AAPE **59**, 6, pp. 968–996

HUTCHINSON I. 1985: The effect of sedimentation and compaction on oceanic heat flow. Geophys. J. R. Astr. Soc. **82**, pp. 439–459

JAPSEN P. 1993: Influence of lithology and Neogene uplift on seismic velocities in Denmark: Implications for depth conversion of maps. AAPG **77**, 2, pp. 194–211

JENSEN P. K., HOLM L., THOMSEN E. 1985: Modelling burial history temperature and maturation. *In*: THOMAS et al.(eds): Petroleum geochemistry in exploration of the Norwegian shelf. Graham & Trotman, London, pp. 145–152

JENSEN P. K. 1988: Preliminary simulations of transformation ratios for the Danish well Aars-1A: Riso-M-2552, Riso National Laboratory, DK-4000, Roskilde, Denmark. 23 p.

LARSEN F. 1986: A sedimentologic and Diagenetic investigation of the Gassum Formation II. Thesis (in Danish) 100 p.

LERCHE I., YARZAB R. F., KENDALL C. G. ST. C. 1984: Determination of Paleoheat flow from vitrinite reflectance data. AAPG **68**, 11, pp. 1704–1717

LERCHE I. 1988a: Inversion of multiple thermal indicators: Quantitative methods of determining paleoheat flux and geological parameters. I. The theoretical development for paleoheat flux. Mathematical Geology **20**, 1, pp. 1–36

LERCHE I. 1988b: Inversion of multiple thermal indicators: Quantitative methods of determining paleoheat flux and geological parameters. II. The theoretical development for chemical, physical and geological parameters. Mathematical Geology **20**, 1, pp. 73–96

MICHELSEN O. (ed) 1982: Geology of the Danish Central Graben. Series B, No. 8. Geological survey of Denmark, 135 p.

MIDDLETON M. F. 1982: The subsidence and thermal history of the Bass basin, South Eastern Australia. Tectonophysics, **87**, pp. 383–397

ROBERTSON E. C. 1979: Thermal conductivities of rocks. Open File Report 79–356, U. S. Geological Survey, 31 p.

SCLATER J. G., CHRISTIE P. A. F. 1980: Continental stretching an explanation of the post-mid-Cretaceous subsidence of the Central North Sea Basin. Journal of Geophysical Research **85**, B7, pp. 3711–3739

SØRENSEN J. P., STEWART W. E. 1980: Structural analysis of multicomponent reaction models: Part 1. Systematic editing of kinetics and thermodynamic values. AIChE Journal **26**, 1, pp. 98–111

SØRENSEN J. P. 1982: Simulation, regression and control of chemical reactors by collocation techniques. Polyteknisk Forlag, Copenhagen Vol. 1.

TISSOT B. P., PELET R., UNGERER P. H. 1987: Thermal history of sedimentary basins, maturation indices, and kinetics of oil and gas generation. AAPG **71**, 12, pp. 1445–1466

THOMSEN E. T. 1984: A coal petrographical investigation of the well Aars-1. Internal report, Geological Survey of Denmark, 22 p.

THOMSEN E. T, DAMTOFT K., ANDERSEN C. 1987: Hydrocarbon plays in Denmark outside the Central Through. *In*: J. BROOKS K. and GLENNIE (eds): Petroleum geology of North West Europe. Graham & Trotman, London, pp. 375–388

UNGERER P., BESSIS F., CHENET P. Y., DURAND B., NOGARET E., CHIARELLI A., OUDIN J. L., PERREN J. F. 1984: Geological and geochemical models in oil exploration; principles and practical examples. AAPG Memoir **35**, pp. 53–77

VEJBÆK O. V. 1989: Effects of asthenospheric heat flow in basin modelling exemplified with the Danish Basin. Earth and Planetary Science Letters, **95**, pp. 97–114

WAPLES D. W. 1980: Time and temperature in petroleum formation: Application of Lopatin's method to petroleum exploration. AAPG **64**, 6, pp. 916–926

YÜKLER M. A., CORNFORD C., WELTE D. 1978: One-dimensional model to simulate geologic, hydrodynamic and thermodynamic development of a sedimentary basin. Geologische Rundschau **67**, 3, pp. 960–979

ØSTFELDT P. 1986: An organic geochemical investigation of the Aars-1. Internal Report, Geological Survey of Denmark

Üledékes medencék feltöltődésének, hőmérsékletének és a szénhidrogén keletkezésének modellezése az Aars-1A (Dánia) mélyfúrás példáján

Peter Klint JENSEN

Egyszerű analitikai kifejezések segítségével számítják ki az Aars-1A dán mélyfúrás feltöltődési és felszín alatti hőmérsékletének alakulását. Az üledékes szekvenciák kompakcióját figyelembe vették. A vitrinit reflektivitást és a szénhidrogén keletkezést egy általános kémiai szimulációs modell segítségével szimulálják. A kémiai reakciók módosításának tekintetében a modell rugalmas. A hőáram történet kiszámítására a mért vitrinit reflektivitás inverziójának módszerét javasolják. A dán Aars-1A mélyfúrásra 1D medence-modellezést készítettek. A 100 millió évvel ezelőttre számított hőáram bizonytalansága (a jelenlegi hőáramhoz viszonyítva) 25%. Ennél korábbi időkre a bizonytalanság tovább növekszik. A Fjerritslev formáció F-III tagjának szénhidrogén keletkezését a geodinamikai modellezésből levezetett hőáramtörténet felhasználásval számították ki.